

pubs.acs.org/NanoLett Letter

# Twin-Directed Deposition of Pt on Pd Icosahedral Nanocrystals for Catalysts with Enhanced Activity and Durability toward Oxygen Reduction

Mingkai Liu, Zhiheng Lyu, Yu Zhang, Ruhui Chen, Minghao Xie, and Younan Xia\*



Cite This: Nano Lett. 2021, 21, 2248-2254



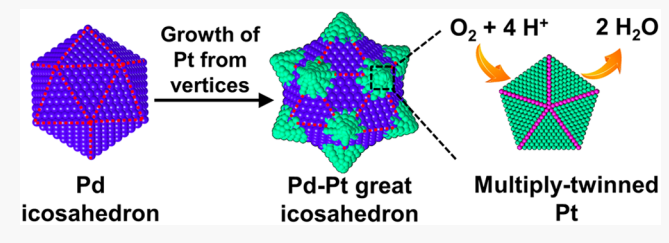
**ACCESS** |

III Metrics & More

Article Recommendations

s Supporting Information

**ABSTRACT:** Platinum nanocrystals featuring a multiply twinned structure and uniform sizes below 5 nm are superb catalytic materials, but it is difficult to synthesize such particles owing to the high twin-boundary energy ( $166 \text{ mJ/m}^2$ ) of Pt. Here, we report a simple route to the synthesis of such nanocrystals by selectively growing them from the vertices of Pd icosahedral seeds. The success of this synthesis critically depends on the introduction of Br $^-$  ions to slow the reduction kinetics of the Pt(II) precursor while limiting the surface diffusion of Pt adatoms by conducting



the synthesis at 30 °C. Owing to the small size and multiply twinned structure of Pt dots, the as-obtained Pd-Pt nanocrystals show remarkably enhanced activity and durability toward oxygen reduction, with a mass activity of 1.23 A mg<sup>-1</sup><sub>Pt</sub> and a specific activity of 0.99 mA cm<sup>-2</sup><sub>Pv</sub> which are 8.2 and 4.5 times as high as those of the commercial Pt/C.

KEYWORDS: icosahedra, multiply twinned structure, bimetallic nanocrystal, twin-induced growth, oxygen reduction

Proton-exchange membrane fuel cells (PEMFCs) are attractive for transportation and many other applications because of their unique capability to provide a clean and consistent source of electricity at high efficiency, low operation temperature, and near-zero emission of harmful gases. 1-3 The effective operation of a PEMFC requires the involvement of a catalyst to mitigate the sluggish kinetics of the reactions, in particular, the oxygen reduction reaction (ORR) on the cathode. The most effective catalyst toward ORR is based upon Pt, but its high cost and low abundance in the earth's crust always present a barrier to the commercialization of PEMFCs on an industrial scale.<sup>4-6</sup> How to reduce the Pt loading of a catalyst without compromising its performance has become a subject of extensive research in recent decades. Most of the endeavors have focused on the development of Pt nanocrystals with uniform and well-controlled sizes and shapes to increase the catalytic activity and thus reduce the loading of this metal.<sup>7-10</sup> In addition, it has been recognized that twin defects can also be utilized to enhance the catalytic activity of Pt nanocrystals by leveraging the surface strains arising from the defects. 11-16 To this end, Pt icosahedral nanocrystals have been identified as a strong candidate for the development of highly active catalysts toward ORR owing to their 12 vertices intersected by five twin boundaries, 30 edges covered by twin boundaries, and 20 side faces featuring compressive strains. 17-20 Although there are a number of reports on the colloidal synthesis of Pt icosahedral nanocrystals, 21 it remains a challenge to generate such a multiply twinned structure with a compact size below 5 nm. As a result, all the Pt icosahedral

nanocrystals reported in the literature tend to suffer from low mass activities because of their low surface-to-volume ratios or small specific surface areas.

Herein, we report a facile route to the synthesis of Pd–Pt great icosahedra featuring multiply twinned Pt dots by confining the nucleation and growth of Pt atoms to the vertices of Pd icosahedral seeds. The success of such a synthesis critically relies on the introduction of Br<sup>-</sup> ions to slow the reduction kinetics of the Pt(II) precursor while decelerating the surface diffusion of the Pt adatoms by lowering the reaction temperature to 30 °C. Owing to their highly twinned structure and strong anchoring to the Pd surface, the Pt dots exhibit significantly enhanced catalytic activity and durability relative to the commercial Pt/C toward oxygen reduction.

Figure 1 illustrates how multiply twinned dots made of Pt are generated by faithfully replicating the vertices of a Pd icosahedral seed. In a typical synthesis, Pd icosahedral nanocrystals with an average diameter of 9.5 nm (see Figure S1) are introduced as seeds to direct the nucleation and growth of Pt under limited-surface diffusion. As one of the key

Received: January 1, 2021 Revised: February 13, 2021 Published: February 18, 2021





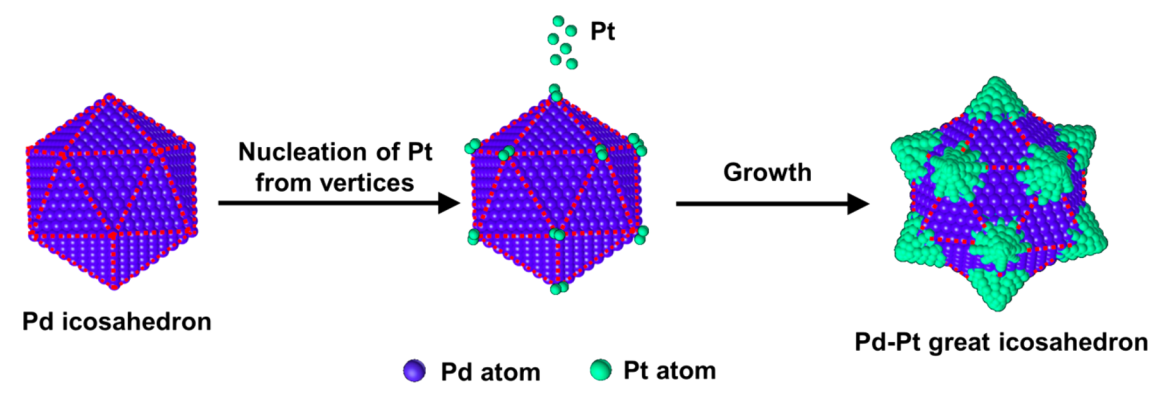


Figure 1. Schematic illustration showing the nucleation and growth of Pt from all the vertices of a Pd icosahedral seed for the formation of a Pd-Pt great icosahedron. The twin boundaries in the Pd seed are marked with red dashed lines.

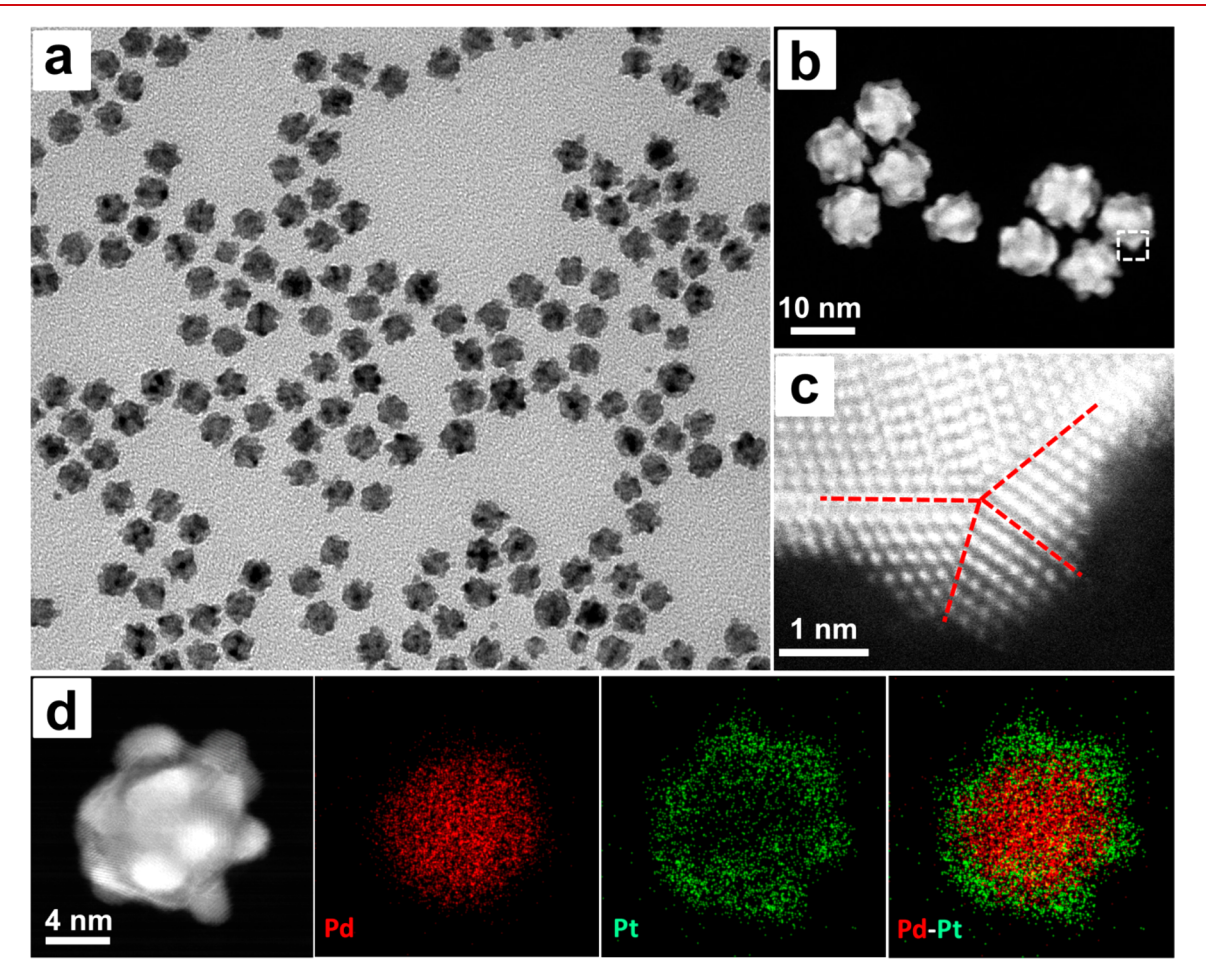


Figure 2. (a) TEM and (b) HAADF-STEM images of the as-obtained Pd—Pt great icosahedra. (c) Atomic-resolution STEM image taken from the corner region of a great icosahedron, as marked by the box in panel (b). The twin boundaries are labeled with red dashed lines. (d) HAADF-STEM image and EDX mapping (red for Pd and green for Pt) of an individual great icosahedron.

requirements, the Pt(II) precursor has to be reduced at a relatively slow rate by adding Br $^-$  ions to transform PtCl $_4$  $^2$  $^-$  into PtBr $_4$  $^2$  $^-$ . Since the vertices of an icosahedron are intersected by five twin boundaries and thus have the highest surface energy, the Pt atoms preferentially nucleate and grow from these sites. We also carry out the synthesis at a temperature as low as 30  $^{\circ}$ C to restrict the surface diffusion of the Pt adatoms from vertices to edges or side faces. Altogether, the Pt atoms derived from the reduction of PtBr $_4$  $^2$  $^-$  are mainly deposited on and confined to the vertices of each

Pd icosahedral seed for the generation of multiply twinned Pt dots. By optimizing the reduction rate of the Pt(II) precursor to avoid symmetry breaking, <sup>22</sup> all the 12 vertices of a Pd icosahedral seed are able to receive Pt atoms, resulting in the formation of a great icosahedron.

Figure 2a shows a representative transmission electron microscopy (TEM) image of the as-prepared sample, in which the Pt dots are clearly observed to protrude from the vertices of each Pd icosahedral seed. The Pt dots have an average size of ca. 3.2 nm (Figure S2). Owing to the introduction of Br<sup>-</sup>

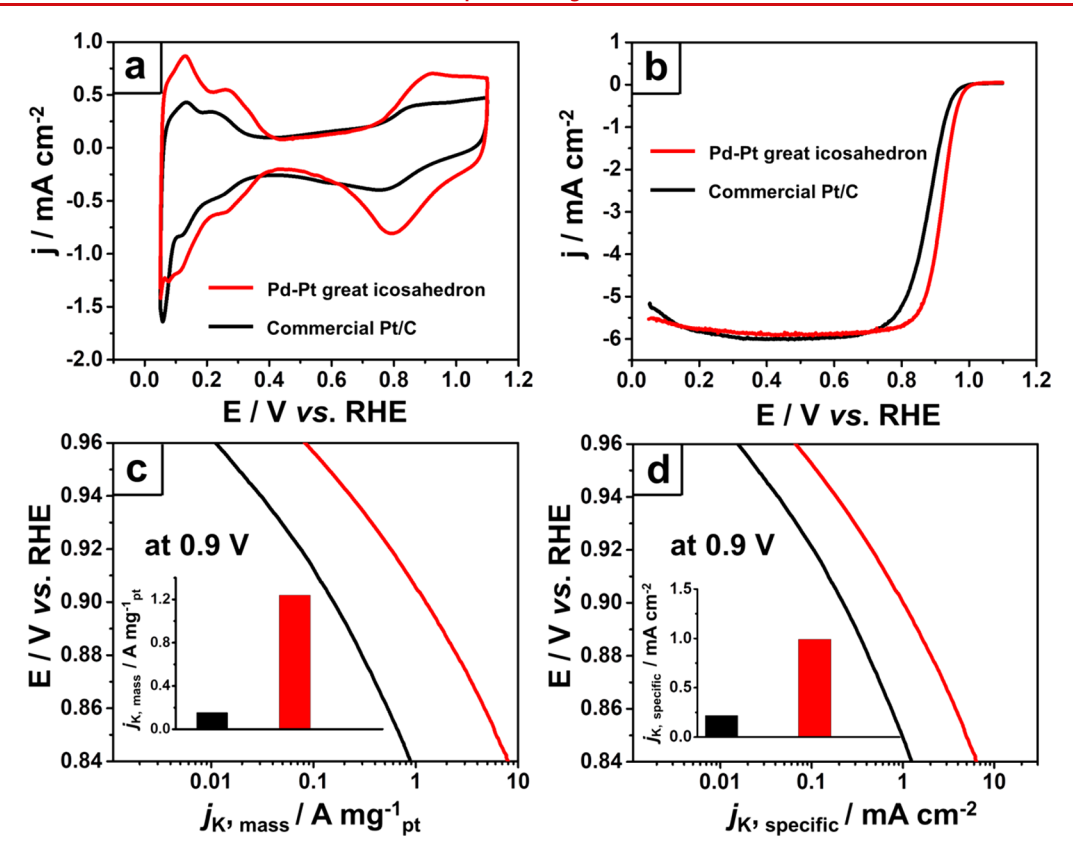


Figure 3. (a) CV curves of the catalysts recorded in a  $N_2$ -saturated HClO<sub>4</sub> solution at room temperature. (b) Polarization curves of the catalysts taken in an  $O_2$ -saturated HClO<sub>4</sub> solution. (c, d) Plots of the (c) mass and (d) specific activities toward oxygen reduction, presented as kinetic current density  $(j_k)$  normalized to the Pt mass and ECSA of the catalyst, respectively. The color scheme in (a) applies to all other panels.

ions and the use of a low reaction temperature to retard both the reduction of the Pt(II) precursor and the surface diffusion of adatoms, the Pt atoms were conformally deposited on the vertices of the Pd icosahedral seeds without involving homogeneous nucleation. Figure 2b shows a high-angle annular dark-field scanning TEM (HAADF-STEM) image of the same sample, revealing the great icosahedral morphology. To further validate the transfer of the twinned structure from the Pd vertex to the Pt dot, we took an atomic-resolution HAADF-STEM image from the region marked by a box in Figure 2b. The image in Figure 2c confirms the presence of multiple twin planes in the Pt dot.

The energy-dispersive X-ray (EDX) mapping of Pd and Pt is shown in Figure 2d, revealing the spatial distributions of these two elements. The mapping data confirms that Pd was mainly confined to the core, while Pt was primarily located in the dots protruding from the vertices of an icosahedral seed. Since it is impossible to completely suppress the surface diffusion of Pt adatoms, a small fraction of them might have diffused to the edges and even side faces, giving some low EDX signals of Pt at these sites. According to the result from an inductively coupled plasma mass spectrometry (ICP-MS) analysis, the Pd-Pt icosahedra synthesized using the standard protocol carried an overall Pt to Pd atomic ratio of 1:4.3. This ratio can be readily tuned by adjusting the amount of the Pt(II) precursor relative to the number of Pd icosahedral seeds. As illustrated in Figure S3, the sizes of the Pt dots increased with the amount of the Pt(II) precursor.

Time-elapsed experiments were also conducted to elucidate the growth mechanism of the Pd—Pt great icosahedra (Figure S4). As the reaction time was extended, the Pt dots were found to protrude more from the vertices of the Pd icosahedral seeds, further verifying the nucleation and growth of Pt dots on all 12 vertices of each seed. This observation confirms that the formation of Pd—Pt great icosahedra followed an atomic deposition mechanism, with no involvement of homogeneous nucleation and particle attachment. This growth mechanism is different from that of another system we reported a while ago, in which Pt nanoparticles were formed through homogeneous nucleation, followed by their attachment to the surface of Pd cuboctahedral seeds for the formation of Pd—Pt dendritic nanostructures.<sup>23</sup> The difference could be largely attributed to the slow reduction kinetics involved in the present work, which favors surface reduction and thus heterogeneous nucleation.<sup>24</sup> The time dependence offers another way to tune the Pt to Pd ratio of the final products.

We further examined the roles of Br<sup>-</sup> ions and reaction temperature in the growth of Pd–Pt great icosahedra. Figure S5 shows TEM images of the products obtained in the absence of Br<sup>-</sup>. Instead of a slightly concave structure for the great icosahedron, dendritic morphology was observed owing to the rapid reduction of PtCl<sub>4</sub><sup>2-</sup> by ascorbic acid and therefore the involvement of homogeneous nucleation and attachment growth. The presence of Br<sup>-</sup> ions and their coordination to the Pt<sup>2+</sup> ions effectively slowed the reduction kinetics of the Pt(II) precursor, ensuring the dominance of surface reduction and heterogeneous nucleation. In the absence of Br<sup>-</sup>, the occurrence of homogeneous nucleation and thereby attachment growth contributed to the formation of a dendritic structure.<sup>23</sup>

Figure S6 shows a TEM image of the Pd-Pt bimetallic nanocrystals prepared under an elevated temperature of 90 °C.

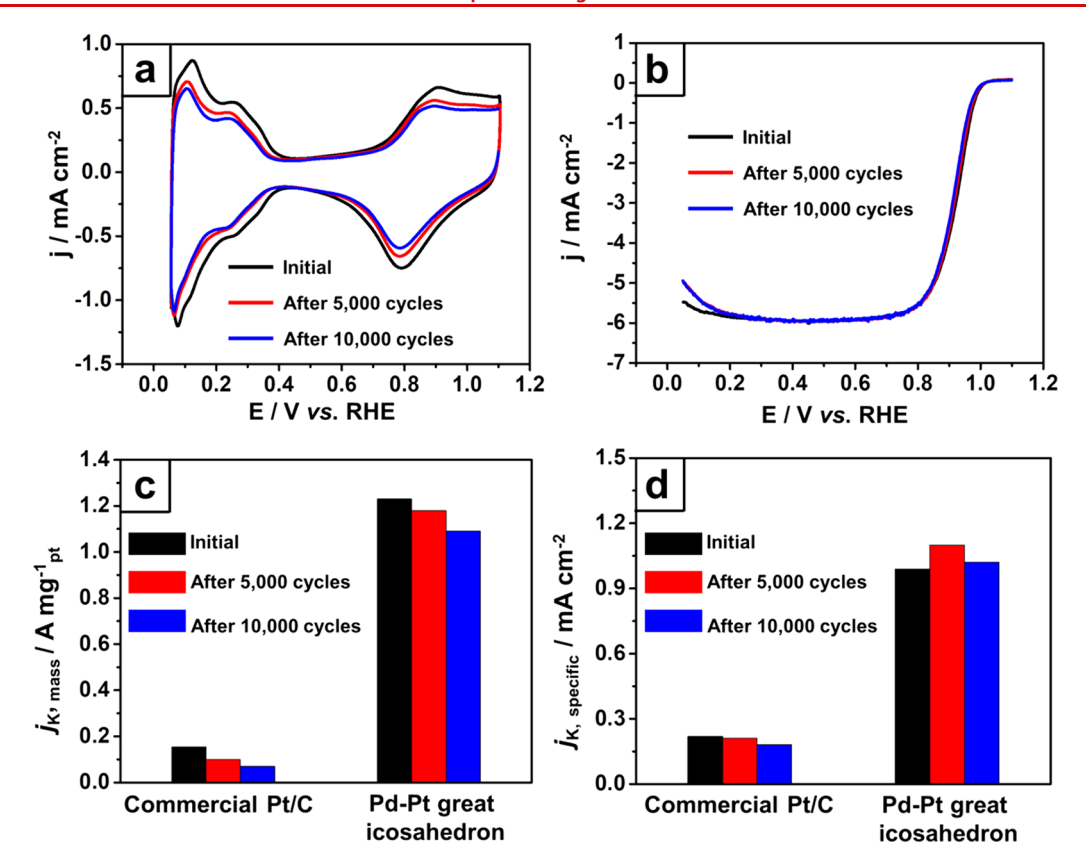


Figure 4. Benchmarking of the Pd—Pt great icosahedra against the commercial Pt/C catalyst. (a) CV and (b) oxygen reduction polarization curves recorded from the Pd—Pt great icosahedra before and after 5000 and 10000 cycles of ADT. (c) Mass and (d) specific activities of the catalysts at  $0.9 \ V_{RHE}$  before and after ADT. The color scheme in (a) applies to all other panels.

Small particles with sizes around 2.5 nm could be easily found in the final products, which could be attributed to the fast reduction and thus homogeneous nucleation of Pt atoms. A similar observation was also made in our previous synthesis of Pd—Pt dendritic nanostructures, where small Pt particles were observed in the initial stage, and they subsequently attached to the surface of the Pd cuboctahedral seeds for the generation of dendritic morphology.<sup>25</sup> Taken together, these results illustrate the multiple roles of lowering the reaction temperature in decelerating the reduction kinetics of the Pt(II) precursor, promoting the surface reduction pathway, suppressing homogeneous nucleation, and impeding surface diffusion.

Finally, we evaluated the catalytic performance of the Pd-Pt great icosahedra toward ORR (Figure 3), together with a comparison to that of the commercial Pt/C catalyst (Figure S7). We used the same type of carbon (Vulcan XC-72, Cabot) in order to minimize the impact of the support. Figure 3a shows the cyclic voltammograms (CVs) of the carbonsupported Pd-Pt great icosahedra and commercial Pt/C. Electrochemical active surface areas (ECSAs) of both catalysts were derived from summing up the charges associated with the desorption of hydrogen and then normalized against the amounts of Pt in the samples. 26-33 Compared to the commercial Pt/C (71.2 m<sup>2</sup> g<sup>-1</sup><sub>pt</sub>), the Pd–Pt great icosahedra exhibited a much higher (almost doubled) ECSA of 124.1 m<sup>2</sup>  $g^{-1}_{\ pt}$  (Table S1). The larger ECSA of the Pd–Pt great icosahedra could be mainly attributed to the better dispersion of the tiny Pt dots and thus the greater utilization efficiency of Pt atoms. Figure 3b shows the polarization curves of the carbon-supported Pd-Pt icosahedra and commercial Pt/C catalyst measured in an O<sub>2</sub>-saturated aqueous HClO<sub>4</sub> solution,

from which the kinetic current density  $(j_k)$  was derived using the Koutecky-Levich equation. The specific  $(j_k)$  specific and mass activities  $(j_k, \text{ mass})$  of the catalyst were obtained by normalizing the  $j_k$  value to the ECSA and the mass of Pt, respectively (Figure 3c and d). The mass activities shown in the inset of Figure 3c at 0.9 V<sub>RHE</sub> indicated that the Pd-Pt great icosahedra were eight times more effective than the Pt/C  $(1.23 \text{ vs } 0.15 \text{ A mg}^{-1}_{Pt})$  in terms of Pt mass. Meanwhile, the specific activity of the Pd-Pt great icosahedra (0.99 mA cm<sup>-2</sup>) was 4.5 times as high as that of the Pt/C  $(0.22 \text{ mA cm}^{-2})$  at 0.9 V<sub>RHE</sub> (inset of Figure 3d). The small size of the Pt dots enabled a larger specific surface area and a higher atom utilization efficiency of Pt, leading to the superior mass activity of Pd-Pt great icosahedra. As shown in Table S2, such a mass activity surpasses most of the previously reported Pd-Pt bimetallic catalysts with various shapes and morphologies. The presence of multiple twin boundaries and the associated surface strain might also contribute to improvement in catalytic performance, similar to the reported high specific activity of Pt icosahedra. 9,11,34-36 The enhanced catalytic activity of the twinned Pt dots can be ascribed to a number of factors. First, the possible incorporation of some Pd atoms in the surface of the as-created Pt dots can reduce the energy barrier to the ratedetermining step of ORR through the ligand and geometric effects. 18 Second, the compressive strain on the regions around the twin boundaries can downshift the d-band center to reduce the adsorption energy between Pt and oxygen intermediates and thus improve the catalytic activity toward ORR.37-

The catalytic stability of the Pd–Pt great icosahedra was also analyzed using an accelerated durability test (ADT) and was benchmarked against the commercial Pt/C. The samples were

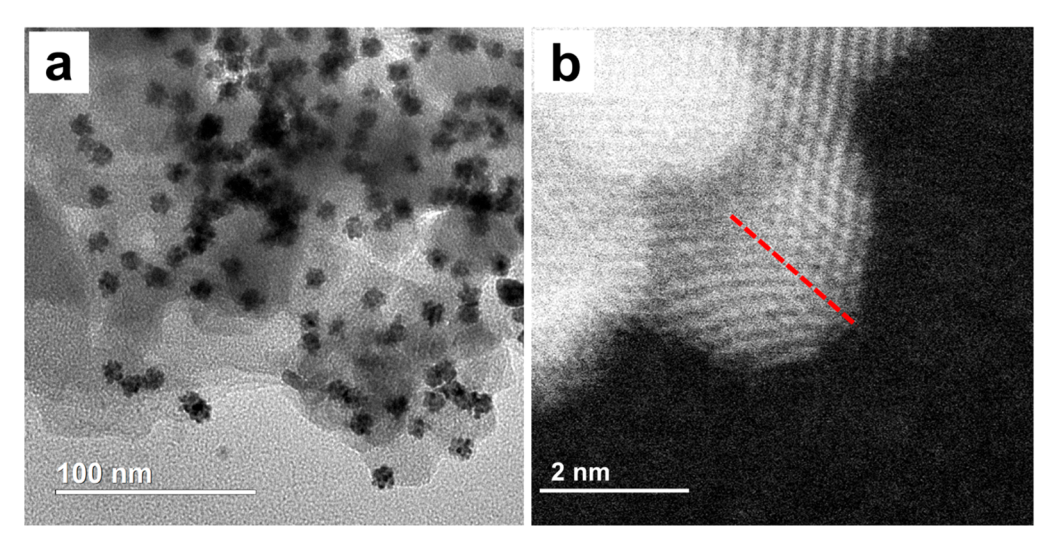


Figure 5. (a) TEM and (b) HAADF-STEM images of the carbon-supported Pd-Pt great icosahedra after 10000 cycles of ADT.

cycled in the range of 0.6-1.1 V<sub>RHE</sub> in an O<sub>2</sub>-saturated HClO<sub>4</sub> solution. After different cycles of ADT, the ECSAs were derived from CV curves of the Pd-Pt great icosahedra (Figure 4a) and Pt/C (Figure S8a). A high value of 106.8 m<sup>2</sup> g<sup>-1</sup><sub>pt</sub> was still obtained for the Pd-Pt great icosahedra after 10000 cycles, which was even higher than the pristine value (71.2 m<sup>2</sup>  $g^{-1}_{pt}$ ) of the Pt/C. Meanwhile, the ECSA of the Pd-Pt icosahedra showed a loss of 13.9% only, much smaller than that of the Pt/C (44.5%). Additionally, the Pd-Pt great icosahedra exhibited a much higher stability with a half-wave potential loss of 0.01 V (Figure 4b) relative to the 0.03 V of the Pt/C (Figure S8b). The mass activity of the Pd-Pt great icosahedra was largely retained at 1.18 and 1.09 A mg<sup>-1</sup><sub>Pt</sub> after 5000 and 10000 cycles (Figure 4c), corresponding to losses of 4.1% and 11.4%, respectively, while that of the Pt/C dropped by 33.3% and 53.3% (0.10 and 0.07 A  $mg^{-1}_{Pt}$ ) under the same ADT conditions (Table S1). All these data confirmed the significantly improved stability of the Pd-Pt great icosahedra. Interestingly, the specific activity of the Pd-Pt great icosahedra was observed to slightly increase to 1.10 mA cm<sup>-2</sup> after 5000 cycles of ADT, relative to the initial value of 0.99 mA cm<sup>-2</sup> (Figure 4d), suggesting the preservation of the twinned structure while presenting surface reconstruction to expose more active sites. To understand the enhancement in durability, we characterized the shape of the Pd-Pt icosahedra after 10000 cycles of ADT using TEM (Figure 5a). The catalytic particles were still well dispersed on the carbon support, with negligible detachment or aggregation. The concave structure and large specific surface area of the great icosahedra enabled more anchoring sites on the carbon support, contributing to their superior stability. Along with the uniform dispersion of the great icosahedral particles, the Pt dots were well separated from each other on the Pd core, helping maintain the high utilization efficiency of the Pt atoms. As shown by the HAADF-STEM image in Figure 5b, the multiply twinned structure of the Pt dot was retained during the 10000 cycles of ADT. In comparison, the small Pt nanoparticles in commercial Pt/C are prone to aggregation after 10000 cycles of ADT (Figure S9), which is consistent with its significant reduction in ECSA (Table S1).

In conclusion, we have demonstrated an effective strategy for the facile synthesis of Pd—Pt great icosahedra decorated with sub-5 nm multiply twinned Pt dots, which showed greatly

enhanced activity and durability toward ORR. By retarding the reduction of the Pt(II) precursor and restricting the surface diffusion, the deposition of Pt atoms could be largely confined to the vertices of the Pd icosahedral seed, leading to the formation of uniform Pt dots with small sizes (ca. 3.2 nm) and a multiply twinned structure. With the leverage of Br ions and a low reaction temperature of 30 °C, the growth of Pt dots followed an atomic deposition route with no involvement of homogeneous nucleation or particle attachment. When evaluated as a catalyst toward ORR and benchmarked against the commercial Pt/C, the Pd-Pt great icosahedra exhibited superior activity and durability. After 10000 cycles of ADT, a 7.3-fold enhancement in mass activity was still achieved for the Pd-Pt great icosahedra relative to the pristine Pt/C due to the preservation of twin boundaries and well-achieved separation of the Pt dots. This synthesis is potentially extendible to other combinations of metals for the development of bimetallic nanocrystals with multiply twinned structures and improved catalytic performance.

# ASSOCIATED CONTENT

## **Solution** Supporting Information

The Supporting Information is available free of charge at https://pubs.acs.org/doi/10.1021/acs.nanolett.1c00007.

Synthetic protocols; TEM image of the Pd icosahedral seeds; size distribution of Pt dots; time-elapsed TEM images of Pd—Pt great icosahedra; TEM images of Pd—Pt nanocrystals synthesized with different amounts of  $K_2PtCl_4$ , without  $Br^-$ , or at a higher temperature; and CV and ORR polarization curves recorded from the commercial Pt/C catalyst before and after different cycles of ADT (PDF)

## AUTHOR INFORMATION

# **Corresponding Author**

Younan Xia — The Wallace H. Coulter Department of Biomedical Engineering, Georgia Institute of Technology and Emory University, Atlanta, Georgia 30332, United States; School of Chemistry and Biochemistry, Georgia Institute of Technology, Atlanta, Georgia 30332, United States; orcid.org/0000-0003-2431-7048; Email: younan.xia@bme.gatech.edu

#### **Authors**

Mingkai Liu — The Wallace H. Coulter Department of Biomedical Engineering, Georgia Institute of Technology and Emory University, Atlanta, Georgia 30332, United States; School of Chemistry and Materials Science, Jiangsu Key Laboratory of Green Synthetic Chemistry for Functional Materials, Jiangsu Normal University, Xuzhou 221116, P. R. China; orcid.org/0000-0001-9060-848X

Zhiheng Lyu — School of Chemistry and Biochemistry, Georgia Institute of Technology, Atlanta, Georgia 30332, United States; oorcid.org/0000-0002-1343-4057

Yu Zhang — The Wallace H. Coulter Department of Biomedical Engineering, Georgia Institute of Technology and Emory University, Atlanta, Georgia 30332, United States; orcid.org/0000-0001-8069-6826

Ruhui Chen – School of Chemistry and Biochemistry, Georgia Institute of Technology, Atlanta, Georgia 30332, United States; Oorcid.org/0000-0003-4163-6964

Minghao Xie — School of Chemistry and Biochemistry, Georgia Institute of Technology, Atlanta, Georgia 30332, United States; orcid.org/0000-0003-3781-5118

Complete contact information is available at: https://pubs.acs.org/10.1021/acs.nanolett.1c00007

#### **Author Contributions**

M.L. prepared and characterized the samples, analyzed the data, and wrote the pristine manuscript. Z.L. took the STEM images. Y.Z. conducted the electrochemical measurements. R.C. and M.X. contributed to data analysis and manuscript revision. Y.X. conceived the concept, supervised the project, and revised the manuscript.

## Notes

The authors declare no competing financial interest.

## ACKNOWLEDGMENTS

This work was supported in part by a grant from the NSF (CHE-1804970). TEM and STEM imaging was performed at the Georgia Tech's Institute for Electronics and Nanotechnology, a member of the National Nanotechnology Coordinated Infrastructure, which is supported by the National Science Foundation (ECCS-1542174).

# **■** REFERENCES

- (1) Greeley, J.; Stephens, I. E. L.; Bondarenko, A. S.; Johansson, T. P.; Hansen, H. A.; Jaramillo, T. F.; Rossmeisl, J.; Chorkendorff, I.; Nørskov, J. K. Alloys of Platinum and Early Transition Metals as Oxygen Reduction Electrocatalysts. *Nat. Chem.* **2009**, *1*, 552–556.
- (2) Huang, H.; Li, K.; Chen, Z.; Luo, L.; Gu, Y.; Zhang, D.; Ma, C.; Si, R.; Yang, J.; Peng, Z.; Zeng, J. Achieving Remarkable Activity and Durability toward Oxygen Reduction Reaction Based on Ultrathin Rh-Doped Pt Nanowires. J. Am. Chem. Soc. 2017, 139, 8152–8159.
- (3) Li, M.; Zhao, Z.; Cheng, T.; Fortunelli, A.; Chen, C.-Y.; Yu, R.; Zhang, Q.; Gu, L.; Merinov, B. V.; Lin, Z.; Zhu, E.; Yu, T.; Jia, Q.; Guo, J.; Zhang, L.; Goddard, W. A.; Huang, Y.; Duan, X. Ultrafine Jagged Platinum Nanowires Enable Ultrahigh Mass Activity for the Oxygen Reduction Reaction. *Science* **2016**, *354*, 1414–1419.
- (4) Yu, T.; Kim, D. Y.; Zhang, H.; Xia, Y. Platinum Concave Nanocubes with High-Index Facets and Their Enhanced Activity for Oxygen Reduction Reaction. *Angew. Chem., Int. Ed.* **2011**, *50*, 2773–2777.
- (5) Rück, M.; Bandarenka, A.; Calle-Vallejo, F.; Gagliardi, A. Oxygen Reduction Reaction: Rapid Prediction of Mass Activity of Nanostructured Platinum Electrocatalysts. *J. Phys. Chem. Lett.* **2018**, *9*, 4463–4468.

- (6) Kumeda, T.; Tajiri, H.; Sakata, O.; Hoshi, N.; Nakamura, M. Effect of Hydrophobic Cations on the Oxygen Reduction Reaction on Single-crystal Platinum Electrodes. *Nat. Commun.* **2018**, *9*, 4378.
- (7) Wang, L.; Holewinski, A.; Wang, C. Prospects of Platinum-Based Nanostructures for the Electrocatalytic Reduction of Oxygen. *ACS Catal.* **2018**, *8*, 9388–9398.
- (8) Ye, W.; Chen, S.; Lin, Y.; Yang, L.; Chen, S.; Zheng, X.; Qi, Z.; Wang, C.; Long, R.; Chen, M.; Zhu, J.; Gao, P.; Song, L.; Jiang, J.; Xiong, Y. Precisely Tuning the Number of Fe Atoms in Clusters on N-Doped Carbon toward Acidic Oxygen Reduction Reaction. *Chem.* 2019, 5, 2865–2878.
- (9) Shao, M.; Peles, A.; Shoemaker, K. Electrocatalysis on Platinum Nanoparticles: Particle Size Effect on Oxygen Reduction Reaction Activity. *Nano Lett.* **2011**, *11*, 3714–3719.
- (10) Cheng, H.; Cao, Z.; Chen, Z.; Zhao, M.; Xie, M.; Lyu, Z.; Zhu, Z.; Chi, M.; Xia, Y. Catalytic System Based on Sub-2 nm Pt Particles and Its Extraordinary Activity and Durability for Oxygen Reduction. *Nano Lett.* **2019**, *19*, 4997–5002.
- (11) Bian, T.; Zhang, H.; Jiang, Y.; Jin, C.; Wu, J.; Yang, H.; Yang, D. Epitaxial Growth of Twinned Au-Pt Core-Shell Star-Shaped Decahedra as Highly Durable Electrocatalysts. *Nano Lett.* **2015**, *15*, 7808–7815.
- (12) Walsh, M. J.; Yoshida, K.; Kuwabara, A.; Pay, M. L.; Gai, P. L.; Boyes, E. D. On the Structural Origin of the Catalytic Properties of Inherently Strained Ultrasmall Decahedral Gold Nanoparticles. *Nano Lett.* **2012**, *12*, 2027–2031.
- (13) Wu, J.; Li, P.; Pan, Y. T.; Warren, S.; Yin, X.; Yang, H. Surface Lattice-engineered Bimetallic Nanoparticles and Their Catalytic Properties. *Chem. Soc. Rev.* **2012**, *41*, 8066–8074.
- (14) Xiong, Y.; McLellan, J. M.; Yin, Y.; Xia, Y. Synthesis of Palladium Icosahedra with Twinned Structure by Blocking Oxidative Etching with Citric Acid or Citrate Ions. *Angew. Chem., Int. Ed.* **2007**, *46*, 790–794.
- (15) Lim, B.; Wang, J.; Camargo, P. H. C.; Cobley, C. M.; Kim, M. J.; Xia, Y. Twin-Induced Growth of Palladium-Platinum Alloy Nanocrystals. *Angew. Chem., Int. Ed.* **2009**, *48*, 6304–6308.
- (16) Zhang, H.; Jin, M.; Xiong, Y.; Lim, B.; Xia, Y. Shape-Controlled Synthesis of Pd Nanocrystals and Their Catalytic Applications. *Acc. Chem. Res.* **2013**, *46*, 1783–1794.
- (17) He, D. S.; He, D.; Wang, J.; Lin, Y.; Yin, P.; Hong, X.; Wu, Y.; Li, Y. Ultrathin Icosahedral Pt-Enriched Nanocage with Excellent Oxygen Reduction Reaction Activity. *J. Am. Chem. Soc.* **2016**, *138*, 1494–1497.
- (18) Wang, X.; Choi, S.-I.; Roling, L. T.; Luo, M.; Ma, C.; Zhang, L.; Chi, M.; Liu, J.; Xie, Z.; Herron, J. A.; Mavrikakis, M.; Xia, Y. Palladium-platinum Core-shell Icosahedra with Substantially Enhanced Activity and Durability Towards Oxygen Reduction. *Nat. Commun.* **2015**, *6*, 7594.
- (19) Wang, X.; Figueroa-Cosme, L.; Yang, X.; Luo, M.; Liu, J.; Xie, Z.; Xia, Y. Pt-Based Icosahedral Nanocages: Using a Combination of {111} Facets, Twin Defects, and Ultrathin Walls to Greatly Enhance Their Activity toward Oxygen Reduction. *Nano Lett.* **2016**, *16*, 1467–1471
- (20) Wang, X.; Vara, M.; Luo, M.; Huang, H.; Ruditskiy, A.; Park, J.; Bao, S.; Liu, J.; Howe, J.; Chi, M.; Xie, Z.; Xia, Y. Pd@Pt Core-Shell Concave Decahedra: A Class of Catalysts for the Oxygen Reduction Reaction with Enhanced Activity and Durability. *J. Am. Chem. Soc.* 2015, 137, 15036–15042.
- (21) Yang, T. H.; Zhou, S.; Gilroy, K. D.; Figueroa-Cosme, L.; Lee, Y. H.; Wu, J. M.; Xia, Y. Autocatalytic Surface Reduction and Its Role in Controlling Seed-mediated Growth of Colloidal Metal Nanocrystals. *Proc. Natl. Acad. Sci. U. S. A.* **2017**, *114*, 13619–13624.
- (22) Zeng, J.; Zhu, C.; Tao, J.; Jin, M.; Zhang, H.; Li, Z.-Y.; Zhu, Y.; Xia, Y. Controlling the Nucleation and Growth of Silver on Palladium Nanocubes by Manipulating the Reaction Kinetics. *Angew. Chem., Int. Ed.* **2012**, *51*, 2354–2358.
- (23) Lim, B.; Jiang, M.; Yu, T.; Camargo, P. H. C.; Xia, Y. Nucleation and Growth Mechanisms for Pd-Pt Bimetallic Nano-

- dendrites and Their Electrocatalytic Properties. Nano Res. 2010, 3, 69-80.
- (24) Xia, X.; Xie, S.; Liu, M.; Peng, H.-C.; Lu, N.; Wang, J.; Kim, M. J.; Xia, Y. On the Role of Surface Diffusion in Determining the Shape or Morphology of Noble-metal Nanocrystals. *Proc. Natl. Acad. Sci. U. S. A.* **2013**, *110*, 6669–6673.
- (25) Lim, B.; Jiang, M.; Camargo, P. H. C.; Cho, E. C.; Tao, J.; Lu, X.; Zhu, Y.; Xia, Y. Pd-Pt Bimetallic Nanodendrites with High Activity for Oxygen Reduction. *Science* **2009**, *324*, 1302–1305.
- (26) Park, J.; Wang, H.; Vara, M.; Xia, Y. Platinum Cubic Nanoframes with Enhanced Catalytic Activity and Durability Toward Oxygen Reduction. *ChemSusChem* **2016**. *9*. 2855–2861.
- (27) Park, J.; Zhang, L.; Choi, S.-I.; Roling, L. T.; Lu, N.; Herron, J. A.; Xie, S.; Wang, J.; Kim, M. J.; Mavrikakis, M.; Xia, Y. Atomic Layer-by-Layer Deposition of Platinum on Palladium Octahedra for Enhanced Catalysts toward the Oxygen Reduction Reaction. ACS Nano 2015, 9, 2635–2647.
- (28) Qian, J.; Shen, M.; Zhou, S.; Lee, C.-T.; Zhao, M.; Lyu, Z.; Hood, Z. D.; Vara, M.; Gilroy, K. D.; Wang, K.; Xia, Y. Synthesis of Pt nanocrystals with Different Shapes Using the Same Protocol to Optimize Their Catalytic Activity Toward Oxygen Reduction. *Mater. Today* 2018, 21, 834–844.
- (29) Hong, J. W.; Kang, S. W.; Choi, B.-S.; Kim, D.; Lee, S. B.; Han, S. W. Controlled Synthesis of Pd-Pt Alloy Hollow Nanostructures with Enhanced Catalytic Activities for Oxygen Reduction. *ACS Nano* **2012**, *6*, 2410–2419.
- (30) Peng, Z.; Yang, H. Synthesis and Oxygen Reduction Electrocatalytic Property of Pt-on-Pd Bimetallic Heteronanostructures. *J. Am. Chem. Soc.* **2009**, *131*, 7542–7543.
- (31) Zhao, X.; Chen, S.; Fang, Z.; Ding, J.; Sang, W.; Wang, Y.; Zhao, J.; Peng, Z.; Zeng, J. Octahedral Pd@Pt<sub>1.8</sub>Ni Core-Shell Nanocrystals with Ultrathin PtNi Alloy Shells as Active Catalysts for Oxygen Reduction Reaction. *J. Am. Chem. Soc.* **2015**, 137, 2804–2807
- (32) Chen, S.; Su, H.; Wang, Y.; Wu, W.; Zeng, J. Size-Controlled Synthesis of Platinum-Copper Hierarchical Trigonal Bipyramid Nanoframes. *Angew. Chem., Int. Ed.* **2015**, *54*, 108–113.
- (33) Wang, W.; Wang, Z.; Wang, J.; Zhong, C.-J.; Liu, C.-J. Highly Active and Stable Pt-Pd Alloy Catalysts Synthesized by Room-Temperature Electron Reduction for Oxygen Reduction Reaction. *Adv. Sci.* **2017**, *4*, 1600486.
- (34) Liu, S.; Mu, X.; Li, W.; Lv, M.; Chen, B.; Chen, C.; Mu, S. Cation Vacancy-modulated PtPdRuTe Five-fold Twinned Nanomaterial for Catalyzing Hydrogen Evolution Reaction. *Nano Energy* **2019**, *61*, 346–351.
- (35) Zhao, M.; Holder, J.; Chen, Z.; Xie, M.; Cao, Z.; Chi, M.; Xia, Y. Facile Synthesis of Pt Icosahedral Nanocrystals with Controllable Sizes for the Evaluation of Size-Dependent Activity toward Oxygen Reduction. *ChemCatChem* **2019**, *11*, 2458–2463.
- (36) Wu, J.; Qi, L.; You, H.; Gross, A.; Li, J.; Yang, H. Icosahedral Platinum Alloy Nanocrystals with Enhanced Electrocatalytic Activities. J. Am. Chem. Soc. 2012, 134, 11880–11883.
- (37) Li, M.; Zhao, Z.; Cheng, T.; Fortunelli, A.; Chen, C.-Y.; Yu, R.; Zhang, Q.; Gu, L.; Merinov, B. V.; Lin, Z.; Zhu, E.; Yu, T.; Jia, Q.; Guo, J.; Zhang, L.; Goddard, W. A.; Huang, Y.; Duan, X. Ultrafine jagged platinum nanowires enable ultrahigh mass activity for the oxygen reduction reaction. *Science* **2016**, *354*, 1414–1419.
- (38) Zhang, Z.; Luo, Z.; Chen, B.; Wei, C.; Zhao, J.; Chen, J.; Zhang, X.; Lai, Z.; Fan, Z.; Tan, C.; Zhao, M.; Lu, Q.; Li, B.; Zong, Y.; Yan, C.; Wang, G.; Xu, Z. J.; Zhang, H. One-Pot Synthesis of Highly Anisotropic Five-Fold-Twinned PtCu Nanoframes Used as a Bifunctional Electrocatalyst for Oxygen Reduction and Methanol Oxidation. *Adv. Mater.* **2016**, *28*, 8712–8717.
- (39) Strasser, P.; Koh, S.; Anniyev, T.; Greeley, J.; More, K.; Yu, C.; Liu, Z.; Kaya, S.; Nordlund, D.; Ogasawara, H.; Toney, M. F.; Nilsson, A. Lattice-strain control of the activity in dealloyed core-shell fuel cell catalysts. *Nat. Chem.* **2010**, *2*, 454–460.

(40) Gu, J.; Zhang, Y.-W.; Tao, F. Shape control of bimetallic nanocatalysts through well-designed colloidal chemistry approaches. *Chem. Soc. Rev.* **2012**, *41*, 8050–8065.